Stem Cell Research & Therapy

RESEARCH Open Access

Fucoxanthin protects placenta-derived human mesenchymal stem cells against oxidative stress-induced apoptosis by modulating genes involved in DNA damage repair, ER stress response, p53-induced apoptosis

Gunticha Suwanmanee[1], Pakpoom Kheolamai[1,2], Chairat Tantrawatpan[1,2], Daniel Grimes[3], Ioan Valentin Matei[4], Luminita Paraoan[4] and Sirikul Manochantr[1,2*]

Abstract

Human mesenchymal stem cells (hMSCs) hold significant promise in regenerative medicine due to their ability to reduce inflammation and promote tissue repair. However, their therapeutic potential is often compromised by their high susceptibility to apoptosis under oxidative stress, prevalent in the microenvironment of the target tissues. Our previous study showed that fucoxanthin, a carotenoid derived from brown algae, can improve the viability of placenta-derived mesenchymal stem cells (PL-MSCs) by reducing intracellular ROS levels through the activation of the PI3K/Akt/Nrf-2 signaling pathway. In this study, we further investigate the mechanisms underlying the protective effect of fucoxanthin against oxidative stress-induced apoptosis in PL-MSCs, using an in vitro model. PL-MSCs were cultured with 750 μM H_2O_2 to induce oxidative stress and treated with various concentrations of fucoxanthin for 48 h. The effect of fucoxanthin on PL-MSC apoptosis under oxidative stress conditions was determined using CCK-8, Annexin V/DRAQ7™ apoptosis assays, as well as the expression of apoptosis-related genes and proteins. The effect of fucoxanthin on the transcriptome of PL-MSCs under oxidative stress conditions was also assessed by high-throughput Nanostring analysis. The results showed that fucoxanthin significantly decreased the apoptosis of PL-MSCs under oxidative stress in a dose-dependent manner by reducing the expression of pro-apoptotic proteins and inhibiting their activation, while increasing the expression of anti-apoptotic proteins in these cells. Furthermore, fucoxanthin also downregulates the expression of genes associated with the endoplasmic reticulum stress, p53-induced apoptosis, while increasing the expression of genes involved in the regulation of the cell cycle, DNA damage repair, cytokine signaling, nucleotide synthesis, PI3K/mTOR pathway and AMPK pathway in PL-MSCs under oxidative stress conditions. Taken together, the findings provide compelling evidence that fucoxanthin protects PL-MSCs against oxidative stress-induced apoptosis by modulating the expression of various genes involved in DNA damage repair, ER stress response, p53-induced apoptosis in these cells. This suggests that

*Correspondence:
Sirikul Manochantr
msirikul@tu.ac.th

Full list of author information is available at the end of the article

fucoxanthin could be used in combination with other agents to increase the therapeutic potential of MSCs by improving their viability under conditions of oxidative stress in the target tissue microenvironment.

Keywords Apoptosis, Biomarkers, Fucoxanthin, Mesenchymal stem cells, Oxidative stress, Placenta

Background

Human mesenchymal stem cells (hMSCs) could potentially be used in cell-based therapies due to their ability to home in on specific tissues and release various beneficial factors to reduce inflammation and promote tissue repair [1, 2]. However, there is evidence indicating that most MSCs undergo apoptosis shortly after being introduced into the target tissues [3, 4]. The poor viability of grafted MSCs is largely due to oxidative stress caused by an excessive amount of reactive oxygen species (ROS) in target tissues [5]. Oxidative stress has been shown to inhibit proliferation, increase senescence, and induce apoptosis in transplanted MSCs by damaging their cellular components [6].

Fucoxanthin, a marine carotenoid derived from edible brown algae, is known for its strong antioxidant properties that provide various health benefits, including anti-obesity [7], anti-cancer [8] and anti-inflammation [9] effects. Previous studies indicate that fucoxanthin significantly increases glutathione levels, reduces ROS, inhibits DNA damage, restores mitochondrial membrane potential and suppresses apoptosis in human keratinocytes [10, 11], retinal pigment epithelial cells [12, 13] and neurons [14] under oxidative stress conditions. Furthermore, our previous study found that fucoxanthin also protects human placenta-derived mesenchymal stem cells (PL-MSCs) from oxidative stress by reducing intracellular ROS production and improving their viability by activating the PI3K/Akt/Nrf-2 signaling pathway [15].

However, the effect of fucoxanthin on the prevention of MSC apoptosis under oxidative stress conditions has not yet been determined. Therefore, in this study, we further investigate the mechanisms underlying the protective effect of fucoxanthin against oxidative stress-induced apoptosis in PL-MSCs. We use PL-MSCs, which can be harvested in large numbers by a non-invasive procedure, and have a higher proliferative and engraftment capacity than bone marrow-derived mesenchymal stem cells (BM-MSCs) [16, 17], as a primary cell type for our investigation.

To study the effects of fucoxanthin on PL-MSC apoptosis under oxidative stress conditions, the percentages of MSC apoptosis, the expression of genes related to apoptosis, and the levels of apoptotic regulator proteins after fucoxanthin treatment were determined. The effect of fucoxanthin on the transcriptome of PL-MSCs under oxidative stress conditions was also studied by high-throughput Nanostring analysis.

Materials and methods

Ethical approval and consent

All experimental procedures were conducted in accordance with the Declaration of Helsinki and the Belmont Report. This study received approval from the Human Research Ethics Committee of Thammasat University (Medicine) under the title 'The effects of fucoxanthin on the proliferation and osteogenic differentiation of human mesenchymal stem cells.' (Approval number: 024/2021) on 4 February 2021. All samples were collected from donors who gave their written informed consent.

Isolation and culture of placental-derived human mesenchymal stem cells

Placental tissues were collected from five healthy volunteers after normal deliveries at the Thammasat University Hospital. The tissues were cut into small pieces and digested by incubation with 0.5% trypsin-EDTA (Gibco, USA) at 37 °C for 2 h. After washing twice with phosphate-buffered saline (PBS), cells were cultured in a complete Dulbecco's modified Eagle's medium (DMEM) supplemented with 10% v/v fetal bovine serum (FBS; Gibco, USA), 1% penicillin/streptomycin, and 1% glutamax (Gibco, USA), at 37 °C in a humidified atmosphere with 5% CO_2. The medium was replaced twice a week. When cultures reached 80–90% confluence, cells were trypsinized with 0.25% (w/v) trypsin/EDTA (Gibco, USA). Cells from passages 3 to 6 were used for all experiments.

Characterization of PL-MSCs

Immunophenotyping

5×10^5 PL-MSCs were incubated with 5 µL fluorescein isothiocyanate (FITC) or phycoerythrin (PE)-conjugated antibodies against human leukocyte antigen – DR isotype (HLA-DR) (Bio Legend, USA), CD34 (Bio Legend, USA), CD45 (Bio Legend, USA), CD73 (Bio Legend, USA), CD90 (BD Biosciences, USA) and CD105 (BD Biosciences, USA) for 30 min at 4 °C in the dark. Subsequently, the cells were fixed with 1% paraformaldehyde in PBS and analyzed using flow cytometry (DxFLEX flow cytometer, Beckman Coulter, USA) with CytExpert software (DxFLEX flow cytometer, Beckman Coulter, USA).

Trilineage differentiation assays

For osteogenic differentiation, PL-MSCs were cultured in complete DMEM in 6-well plates (Corning, USA) at a density of 4.5×10^3 cells/cm^2 overnight. Subsequently, the medium was replaced with osteogenic differentiation

medium, a complete DMEM supplemented with 100 nM dexamethasone and 50 µg/mL ascorbic acid (Sigma-Aldrich, USA). On day 7, 10 µM β-glycerophosphate (Sigma-Aldrich, USA) was added to the osteogenic differentiation medium and the cells were cultured for an additional 3 weeks, with medium replacements every 3–4 days. On day 28, cells were fixed, stained with 40 mM Alizarin red S (Sigma-Aldrich, USA) for 30 min at room temperature, and observed by light microscopy (Nikon Eclipse Ts2R, Japan).

For adipogenic differentiation, PL-MSCs were cultured in adipogenic differentiation medium, a complete DMEM supplemented with 100 µM indomethacin, 25 mM glucose, 1 µM dexamethasone, and 1 µg/mL insulin (all purchased from Sigma-Aldrich, USA) for 28 days. On day 28 of culture, cells were fixed with 37% formalin vapor for 20 min, stained with 0.5% Oil red O (Sigma-Aldrich, USA) in 6% isopropanol for 20 min at room temperature and observed under an inverted light microscope.

For chondrogenic differentiation, PL-MSCs were cultured in a 96-well U-bottom plate (Jet Biofil, China) containing complete DMEM at a density of 3×10^4 cells/cm^2 overnight to generate spheroids. Subsequently, the medium was replaced with MSCgo™ Chondrogenic XF medium (Sartorius, Germany); spheroids were cultured for an additional 3 weeks. At the end of the culture, spheroids were fixed with 10% formalin for 30 min, stained with 1% Alcian blue (HiMedia, India) in 0.1 M HCl at room temperature overnight, in the dark, washed twice with 0.1 M HCl and observed by stereoscopic microscopy. In all differentiation experiments, PL-MSCs cultured in complete DMEM served as controls.

CCK-8 cell viability assay

Cytotoxicity was determined using the cell counting kit-8 (CCK-8) assay (Dojindo Laboratories, Japan). Briefly, PL-MSCs were seeded in a 96-well plate (Corning, USA) at a density of 3×10^4 cells/cm^2. Cells were then treated with fucoxanthin (Sigma-Aldrich, USA) at final concentrations of 1, 2, 3, 4, 5, 10, and 20 µM for 48 h. At 24 and 48 h after treatment, 10 µL of CCK-8 solution was added to each well and cells were incubated at 37 °C for 4 h. After incubation, absorbance was measured at 450 nm using an Agilent BioTek Synergy H1 Multimode Reader; analysed with Agilent BioTek Gen5 software version 3.14 (BioTek Instruments Inc., USA). Cell viability was presented as percentage of control, calculated using the following equation.

$$\text{Cell viability } (\%\text{ of control}) = \left(\frac{\text{OD (test)} - \text{OD (blank)}}{\text{OD (control)} - \text{OD (blank)}}\right) \times 100$$

H_2O_2-induced oxidative stress

To induce oxidative stress, PL-MSCs were seeded in a 96-well plate (Corning, USA) at a density of 3×10^4 cells/cm^2 and treated with 50-1500 µM H_2O_2 (Sigma-Aldrich; Merck Millipore, Germany) in a complete DMEM at 37 °C for 24 h. Cell viability was assessed using a CCK-8 assay as described above.

MTT assay

To assess the effects of fucoxanthin on PL-MSCs under acute oxidative stress to mimic the environment in damaged tissues, PL-MSCs were seeded in 96-well plates (Corning, USA) at 3×10^4 cells/cm² and treated with 750 µM H_2O_2 and fucoxanthin (1–5 µM) for 24 and 48 h. Untreated PL-MSCs cultured in complete DMEM served as controls. Cell viability was assessed using the 3- (4, 5-dimethylthiazol-2-yl) -2,5-diphenyltetrazolium bromide (MTT) assay (Sigma-Aldrich, USA). The absorbance was measured at 570 nm using a Synergy HT Multi-Detection Microplate Reader and Agilent BioTek Gen6 software (BioTek Instruments Inc., USA). Cell viability was calculated as shown in the equation:

$$\text{Cell viability } (\%\text{ of control}) = \frac{\text{OD (test)} - \text{OD (blank)} \times 100}{\text{OD (control)} - \text{OD (blank)}}$$

Apoptosis assay

The percentage of cell apoptosis was measured using the Annexin V-FITC / DRAQ7™ apoptosis assay (Abcam, USA) according to the manufacturer's protocol. Briefly, PL-MSCs were seeded in a 6-well plate (Corning, USA) at a density of 1.5×10^4 cells/cm^2 and co-treated with 750 µM H_2O_2 and 1–5 µM fucoxanthin for 24 h. PL-MSCs treated with H_2O_2 without fucoxanthin supplementation for 24 h served as controls. After treatment, cells were harvested, labeled with 5 µM Annexin V-FITC and DRAQ7™ in 200 µL cold labeling buffer for 15 min, protected from light, and, apoptosis was determined using BD FACSMelody™ flow cytometer (BD Biosciences, USA) followed by analysis with FlowJo™ software (BD Biosciences, USA). Total percentage of apoptosis profiles was determined as follows: Live (-) Annexin V-FITC; (-) Draq7, Early apoptosis (+) Annexin V-FITC; (-) Draq7, Late apoptosis (+) Annexin V-FITC; (+) Draq7. Dead (-) Annexin V-FITC; (+) Draq7.

$$\text{Total apoptotic cells } (\%) = \%\text{ early apoptotic cells (Q3)} + \%\text{ late apoptotic cells (Q2)}$$

Gene expression analysis by quantitative real-time polymerase chain reaction (qRT-PCR)

To investigate the expression levels of genes related to apoptosis in PL-MSCs under oxidative stress conditions,

PL-MSCs were treated with 750 μM H_2O_2 and 1–5 μM fucoxanthin for 24 h at 37 °C. Total RNA was isolated using the RNeasy® Mini Kit (Qiagen, Germany) and 1 μg of RNA was reverse transcribed using a High-Capacity RNA-to-cDNA™ Kit (Applied Biosystems; Thermo Fisher Scientific, USA) to generate cDNA according to the manufacturer's instructions. qRT-PCR was performed for 40 cycles using PowerTrack™ SYBR Green Master Mix (Applied Biosystems; Thermo Fisher Scientific, USA). and CT values determined using QuantStudio™ 5 Real-Time PCR System (Applied Biosystems; Thermo Fisher Scientific, USA). All reactions were carried out in triplicate ($n = 3$) and analysed using Design & Analysis 2 (DA2) software version 2.6.0 (Applied Biosystems; Thermo Fisher Scientific, USA). The expression levels of the target genes were normalized to glyceraldehyde-3-phosphate dehydrogenase (*GAPDH*) and presented as relative fold change compared to untreated controls using the $2^{-\Delta\Delta Ct}$ method.

Protein isolation and Western blot analysis

The levels of proteins associated with the intrinsic and extrinsic apoptotic pathway in PL-MSCs under oxidative stress conditions were determined by Western blot analysis. Total protein was isolated using cold RIPA buffer (Sigma-Aldrich, USA) containing protease inhibitor cocktail (Cell Signaling Technology, USA). Total protein concentrations were determined using Pierce® BCA Protein Assay Kit (Thermo Fisher Scientific, USA). 20 μg total protein containing Laemmli sample buffer supplemented with 2-mercaptoethanol (1.43 M) was separated by 12% sodium dodecyl sulfate-polyacrylamide gel electrophoresis (SDS-PAGE; Bio-Rad, USA) and transferred to a nitrocellulose membrane (0.45 μm pore-size; Bio-Rad, USA) using a mini trans-blot electrophoretic transfer cell (Bio-Rad, USA). Subsequently, the membranes were blocked with 1X Pierce™ Clear Milk Blocking Buffer in Tris-buffered saline with 0.1% Tween 20 (TBST) for 2 h at room temperature. Then, the membranes were incubated overnight at 4 °C with gentle agitation in the following primary antibodies: rabbit anti-human caspase 3, rabbit anti-human cleaved-caspase 3, rabbit anti-human caspase 7, rabbit anti-human cleaved-caspase 7, rabbit anti-human caspase 8, rabbit anti-human cleaved-caspase 8, mouse anti-human caspase 9, rabbit anti-human cleaved-caspase 9, rabbit anti-human PARP, rabbit anti-human cleaved-PARP, rabbit anti-human DR4, rabbit anti-human FADD, rabbit anti-human phospho-FADD, rabbit anti-human β-actin, (all from Cell Signaling Technology, USA; diluted 1:1000 in blocking buffer). Following primary antibody incubation, membranes were washed with 0.05% TBST and incubated at room temperature with either goat anti-rabbit or horse anti-mouse horseradish peroxidase (HRP) conjugated secondary antibody (1:2000) (Cell Signaling Technology, USA) in 0.05% TBST for 1 h, gently rocked. Following secondary antibody incubation, membranes were washed again in 0.05% TBST and protein expression was determined using enhanced chemiluminescence (ECL) with Clarity™ Western ECL Substrate (Bio-Rad, USA), detected using a ChemiDoc™ MP Imaging System (Bio-Rad, USA). Membranes were then stripped with stripping buffer (0.5 M Tris HCl, pH 6.8; 2% SDS; 100 mM 2-mercaptoethanol) at 60 °C for 1 h. Protein signal intensity was quantified using NIH ImageJ software and expressed as a fold-change relative to β-actin.

Nanostring® nCounter analysis

The effect of fucoxanthin on the transcriptome of PL-MSCs under oxidative stress conditions was investigated by NanoString® nCounter Technology (NanoString Technologies, Seattle, WA, USA). The PL-MSCs were treated with 750 μM H_2O_2 and 5 μM fucoxanthin for 24 h. Total RNA was isolated using the PureLink™ RNA Mini Kit (Ambion, USA). 100 ng of RNA were hybridized with nCounter Reporter and Capture probes at 65 °C overnight. After hybridization, samples were processed using the nCounter Prep Station to purify and immobilize the target/probe complex onto the cartridge. The nCounter digital analyzer was then used to perform a high-density scan to measure the abundance of target RNA molecules in each sample. Multiplexed gene expression analysis of 768 genes in 34 annotated pathways that are essential for biosynthesis, nutrient capture, anabolic metabolism, catabolic metabolism, cell stress, metabolic signaling, and transcriptional regulation was performed by nSolver software, version 4.0 (NanoString Technologies, Seattle, WA, USA). The mRNA copy numbers were standardized using the geometric mean of 20 housekeeping genes for baseline normalization. A threshold count value of 50 was applied as the baseline subtraction parameter and the changes in gene expression levels were calculated by comparing the fucoxanthin-treated samples with the untreated controls (PL-MSCs treated with 750 μM H_2O_2 without fucoxanthin supplementation).

The differential expression of genes (DEGs) was represented as volcano plots, showing individual genes with -log10 (*p*-value) plotted against log2 fold change relative to a pairwise comparison between (A) PL-MSCs treated with H_2O_2 and untreated control and (B) PL-MSCs treated with a combination of H_2O_2 and fucoxanthin and PL-MSCs treated with H_2O_2 alone. The Kyoto Encyclopedia of Genes and Genomes (KEGG), Gene Ontology (GO) enrichment, and protein-protein interaction (PPI) analysis were performed through the String database using ShinyGO V0.82 [18] to assess functional and pathway enrichment of the DEGs. A Venn diagram visualizing overlapping DEG sets was generated using Venny2.1

(https://bioinfogp.cnb.csic.es/tools/venny/). Transcription factor (TF) regulatory networks were predicted using TRRUST version 2 (https://www.grnpedia.org/trrust/) [19] and validated using STRING version 12.0 (https://string-db.org/) to map protein associations. Statistical significance for enriched terms, pathways, and interactions was defined as $p < 0.05$.

Statistical analysis

Data were presented as the mean ± standard error of the mean (SEM). Significant differences between groups were determined by paired t-test, using SPSS software version 25 (SPSS, Inc.). A p-value of less than 0.05 was considered statistically significant.

Results

Characterization of PL-MSCs

Mesenchymal stem cells derived from the human placenta exhibited spindle-shaped morphology (Fig. 1A) expressed typical MSC surface markers at very high percentages, CD73 (99.04 ± 1.20%), CD90 (98.71 ± 0.52%), and CD105 (99.44 ± 0.50%), and did not express hematopoietic stem cell surface markers CD34, CD45 and HLA-DR (Fig. 1B). These PL-MSCs also have trilineage differentiation capacity toward osteocytes (Fig. 1C), adipocytes (Fig. 1D) and chondrocytes (Fig. 1E) after being induced by appropriate culture conditions, as demonstrated by Alizarin red S staining, Oil-red O staining and Alcian blue staining, respectively.

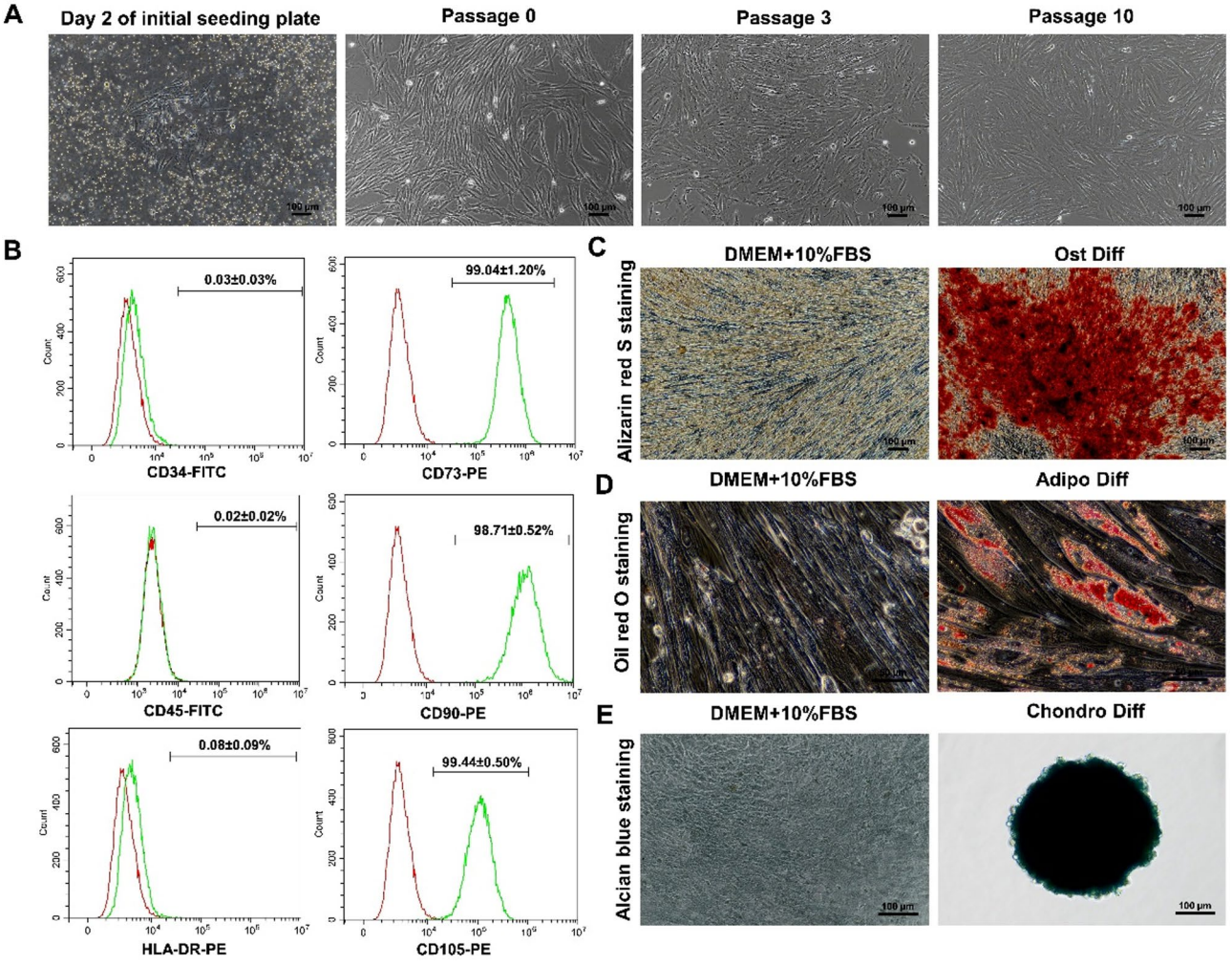

Fig. 1 Characteristics of MSCs derived from human placentas (PL-MSCs). **A** Morphology of PL-MSCs cultured in DMEM supplemented with 10% FBS at day 2 after initial seeding, passage 0, passage 3, and passage 10. Cells retained a spindle-shaped morphology across passages, with no signs of replicative senescence. **B** Flow cytometry confirmed that PL-MSCs were positive for MSC surface markers (CD73, CD90, CD105) and negative for hematopoietic lineage markers (CD34, CD45, HLA-DR). **C** Osteogenic differentiation demonstrated by Alizarin Red S staining (orange-red calcium deposits) after 28 days of induction. **D** Adipogenic differentiation revealed by Oil Red O staining (red lipid droplets) in cytoplasmic vacuoles. **E** Chondrogenic differentiation is shown by Alcian Blue staining (blue proteoglycan-rich matrix). $n = 5$, Images (**A**), (**C**), and (**E**) were taken at 10X, 10X, and 20X, respectively; scale bar = 100 µm. Image **D** was taken at 40X; scale bar = 50 µm

Cytotoxic effect of fucoxanthin on PL-MSCs

We first determined the cytotoxic effects of fucoxanthin on PL-MSCs using the CCK-8 assay. Treatment of PL-MSCs with fucoxanthin at concentrations of up to 5 µM increased their viability at 24 and 48 h compared to untreated control, while 10 and 20 µM fucoxanthin significantly decreased the viability of PL-MSCs at 24 and 48 h compared to untreated control (Fig. 2A). The half-maximal inhibitory concentration (IC_{50}) of fucoxanthin in PL-MSCs was 14.39 ± 4.0 µM after 24 h and 7.81 ± 0.2 µM after 48 h of treatment. Therefore, a fucoxanthin concentration up to 5 µM was chosen for subsequent experiments to avoid any cytotoxic effects.

Fucoxanthin decreases PL-MSC apoptosis under oxidative stress conditions

To establish an in vitro model of oxidative stress, the PL-MSCs were treated with H_2O_2 at concentrations ranging from 50 to 1500 µM for 24 h. The results of the CCK-8 assay showed that H_2O_2 decreased the viability of PL-MSCs in a dose-dependent manner (Fig. 2B) and H_2O_2 at a concentration of 750 µM, which reduces the

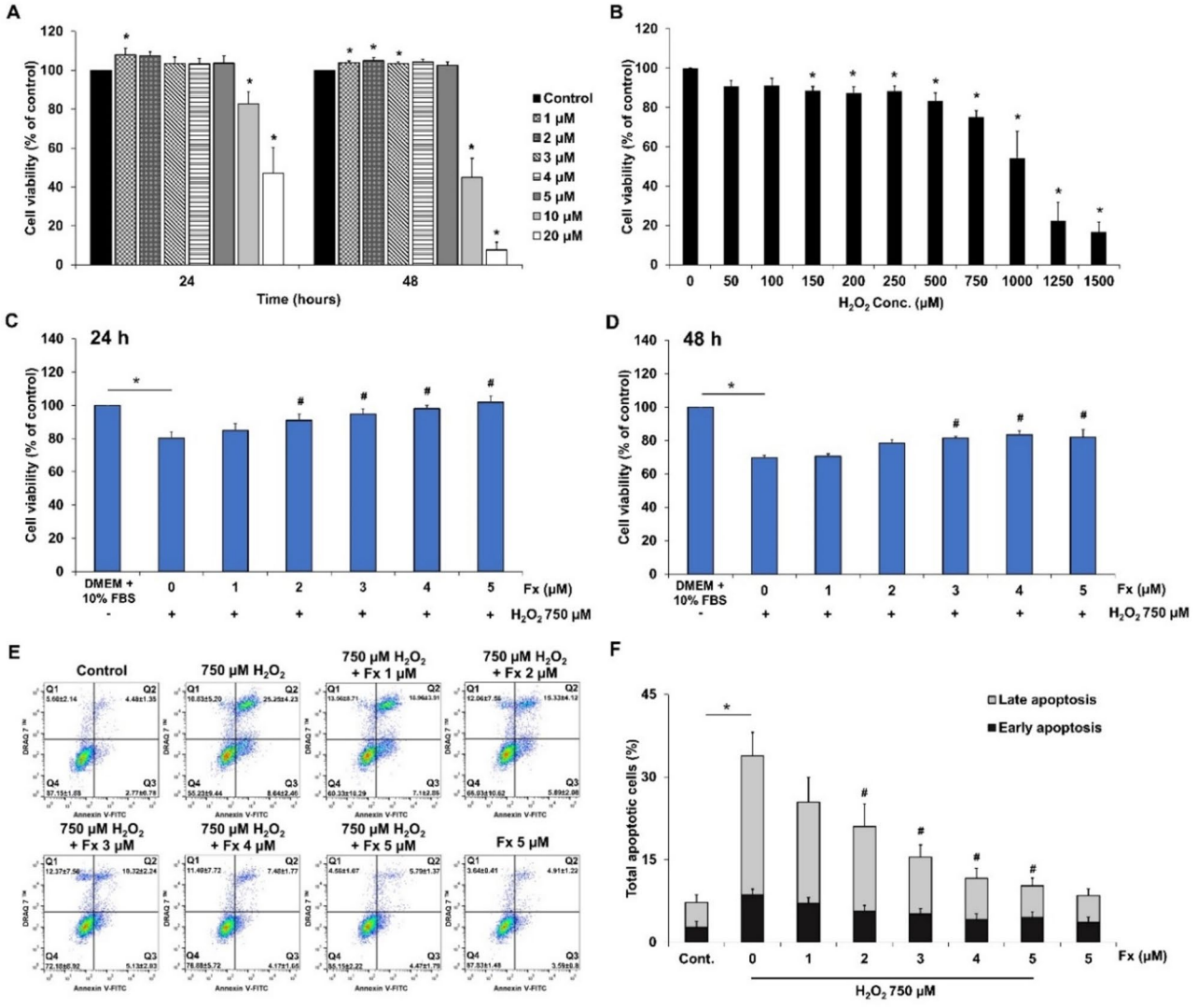

Fig. 2 Cytotoxicity of fucoxanthin and H2O2 on PL-MSCs. (**A**) The CCK-8 assay showed the viability of PL-MSCs treated with increasing concentrations of fucoxanthin (1, 2, 3, 4, 5, 10, and 20 µM) for 24 and 48 h. (**B**) The viability of PL-MSCs treated with H_2O_2 (ranging from 50-1500 µM) for 24 h was evaluated using the CCK-8 assay. (**C**) The viability of PL-MSCs after 24 h of treatment with 750 µM H_2O_2 and fucoxanthin (1-5 µM). (**D**) The viability of PL-MSCs after 48 h of treatment with 750 µM H2O2 and fucoxanthin (1-5 µM). (**E**) Flow cytometry scatter plots categorizing live (Annexin V^-/DRAQ7^{TM-}, Q4), early apoptotic (Annexin V^+/DRAQ7^{TM-}, Q3), and late apoptotic (Annexin V^+/DRAQ7^{TM+}, Q2) in PL-MSCs following 24-h treatment with 750 µM H_2O_2 and fucoxanthin (1–5 µM). (**F**) Quantification of early and late apoptotic PL-MSCs under H_2O_2 and fucoxanthin treatment. Data are presented as mean ± SEM (n = 4). Statistical significance was assessed using the paired t-test. *$p \leq 0.05$ compared to the control (PL-MSCs cultured in complete DMEM), while #$p \leq 0.05$ compared to H_2O_2-treated PL-MSCs without fucoxanthin.

viability of PL-MSCs to 75%, was chosen for subsequent experiments.

Treatment with 750 μM H_2O_2 for 24 h significantly reduced PL-MSC viability compared to untreated controls. However, treatment with increasing fucoxanthin concentrations (1–5 μM) progressively restored viability, with 2–5 μM fucoxanthin showing statistically significant recovery ($p \leq 0.05$). Remarkably, 5 μM fucoxanthin fully restored viability to control levels (101.82% ± 3.71) (Fig. 2C). Similarly, after 48 h of H_2O_2 exposure, viability was significantly reduced but improved dose-dependently with fucoxanthin. A significant increase ($p \leq 0.05$) occurred at 3–5 μM fucoxanthin, achieving 82.09% ± 4.47 viability relative to controls (Fig. 2D). Antioxidant effects of fucoxanthin were further confirmed by reduced intracellular ROS levels in H_2O_2-treated PL-MSCs, as measured by DCFH-DA fluorescence (Supplementary Fig. S1).

To determine the cytoprotective effects of fucoxanthin against oxidative stress-induced apoptosis in PL-MSC, PL-MSCs were co-treated with 750 μM H_2O_2 and 1–5 μM fucoxanthin for 24 h. The percentage of apoptosis was determined by the Annexin V-FITC and DRAQ7™ apoptosis assay. As expected, H_2O_2 treatment significantly increased the percentage of total apoptotic populations, early apoptotic (Annexin V^+/ $DRAQ7^-$), and late apoptotic (Annexin V^+/ $DRAQ7^+$) in PL-MSCs compared to the untreated control (Fig. 2E-F).

Fucoxanthin treatment significantly decreased PL-MSC apoptosis under oxidative stress conditions in a dose-dependent manner compared to control (PL-MSCs treated with 750 μM H_2O_2 without fucoxanthin supplementation) (Fig. 2E-F). Furthermore, 5 μM fucoxanthin treatment reduced PL-MSC apoptosis under the oxidative stress conditions compared to control (PL-MSCs without H_2O_2 treatment) (Fig. 2E-F).

Fucoxanthin decreased the expression of pro-apoptotic genes and increased the expression of anti-apoptotic genes in PL-MSCs under oxidative stress conditions

To determine the effects of fucoxanthin on the expression levels of genes related to apoptosis in PL-MSCs under oxidative stress conditions, PL-MSCs were co-treated with 750 μM H_2O_2 and 1–5 μM fucoxanthin for 24 h. Following treatments, expression levels of pro- and anti-apoptotic genes in PL-MSCs were determined by qRT-PCR. Consistent with its effect on PL-MSC apoptosis, H_2O_2 treatment significantly increased the expression levels of many pro-apoptotic genes in PL-MSCs including Caspase 3 (*CASP3*), Caspase 8 (*CASP8*), Apoptotic protease activating factor 1 (*APAF-1*), Cytochrome c (*CYC C*), BH3 interacting-domain death agonist (*BID*), BCL-2 associated agonist of cell death (*BAD*), BCL-2–associated X (*BAX*), Fas-associated death domain (*FADD*), Tumor necrosis factor receptor superfamily member 10 A (*TNFRSF10A*), and Tumor necrosis factor receptor superfamily member 10B (*TNFRSF10B*), while decreasing the expression levels of anti-apoptotic genes, B-cell lymphoma *2 (BCL-2)* and Survivin (*BIRC5*) compared to the untreated controls (Fig. 3).

To ascertain the mechanistic basis of the positive effects of fucoxanthin on the survival of PL-MSCs, its effects on these key regulatory pro- and anti-apoptotic genes were also ascertained following H_2O_2 treatment. Fucoxanthin significantly decreased the expression levels of pro-apoptotic genes, *CASP3*, *CASP8*, *APAF-1*, *CYC C*,

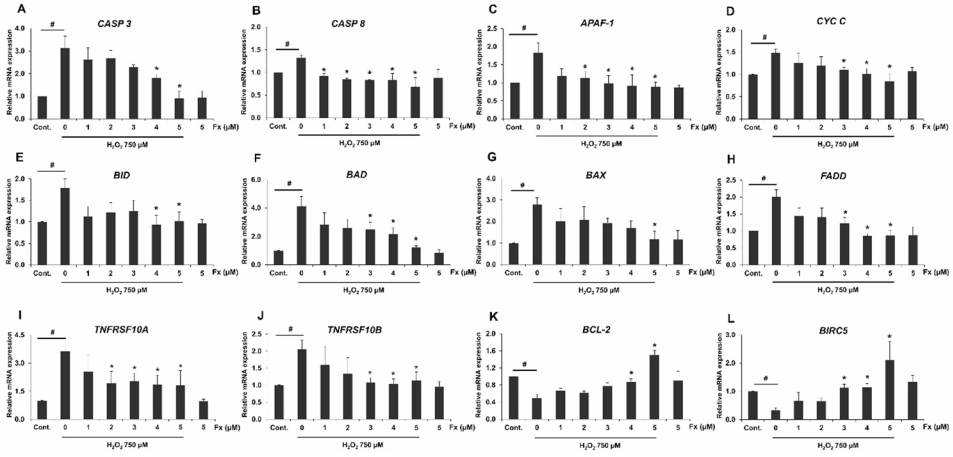

Fig. 3 Effects of fucoxanthin on apoptotic gene expression in H_2O_2-treated PL-MSCs. Quantitative real-time RT-PCR analysis revealed the downregulation in the expression levels of pro-apoptotic genes, including *CASP3* (**A**), *CASP8* (**B**), *APAF-1* (**C**), *CYC C* (**D**), *BID* (**E**), *BAD* (**F**), *BAX* (**G**), *FADD* (**H**), *TNFRSF10A* (***I***), and *TNFRSF10B* (**J**) in PL-MSCs after treatment with 750 μM H_2O_2 and fucoxanthin at 1–5 μM for 24 h. Upregulation in the expression levels of anti-apoptotic genes, *BCL-2* (**K**), and *BIRC5* (**L**) was detected under the same treatment conditions. Data are presented as mean ± SEM, with $n = 3$. Statistical significance was evaluated using a paired t-test, with $^{\#}p \leq 0.05$ indicating significance compared to PL-MSCs cultured in complete DMEM and $^{*}p \leq 0.05$ indicating significance compared to H_2O_2-treated PL-MSCs without fucoxanthin

BID, *BAD*, *BAX*, *FADD*, *TNFRSF10A* and *TNFRSF10B* (Fig. 3A-J), while increasing the expression levels of anti-apoptotic genes, *BCL-2* and *BIRC5* (Fig. 3K-L) in PL-MSC compared to controls (PL-MSCs treated with 750 μM H_2O_2 without fucoxanthin supplementation) in a dose-dependent manner. These findings suggest that fucoxanthin reduces PL-MSC apoptosis under oxidative stress conditions by decreasing the expression of several pro-apoptotic genes and increasing the expression of anti-apoptotic genes.

Fucoxanthin decreases the expression and inhibits the activation of several proteins related to extrinsic and intrinsic apoptotic pathways in PL-MSCs under oxidative stress conditions

The levels of proteins involved in the extrinsic and intrinsic apoptotic pathways in PL-MSCs treated with 750 μM H_2O_2 with or without fucoxanthin supplementation were determined by Western blot analysis. Similar to its effect on pro-apoptotic gene expression, H_2O_2 treatment activated an extrinsic apoptotic pathway in PL-MSCs, as demonstrated by an increase in ratios of phosphorylated Fas-associated death domain (p-FADD) / total Fas-associated death domain (FADD) protein, and cleaved caspase 8/total caspase 8 protein, compared to untreated control.

Consistent with its positive effect on PL-MSC survival, fucoxanthin prevented the activation of the extrinsic apoptotic pathway in PL-MSCs under oxidative stress conditions by significantly decreasing p-FADD/total FADD, and cleaved caspase 8/total caspase 8 protein ratios in H_2O_2-treated PL-MSCs compared to controls (PL-MSCs treated with 750 μM H_2O_2) in a dose-dependent manner (Fig. 4A, C-E; Supplementary Fig. S2-S4). In addition to its inhibitory effect on the extrinsic apoptotic pathway, fucoxanthin also inhibited the activation of the

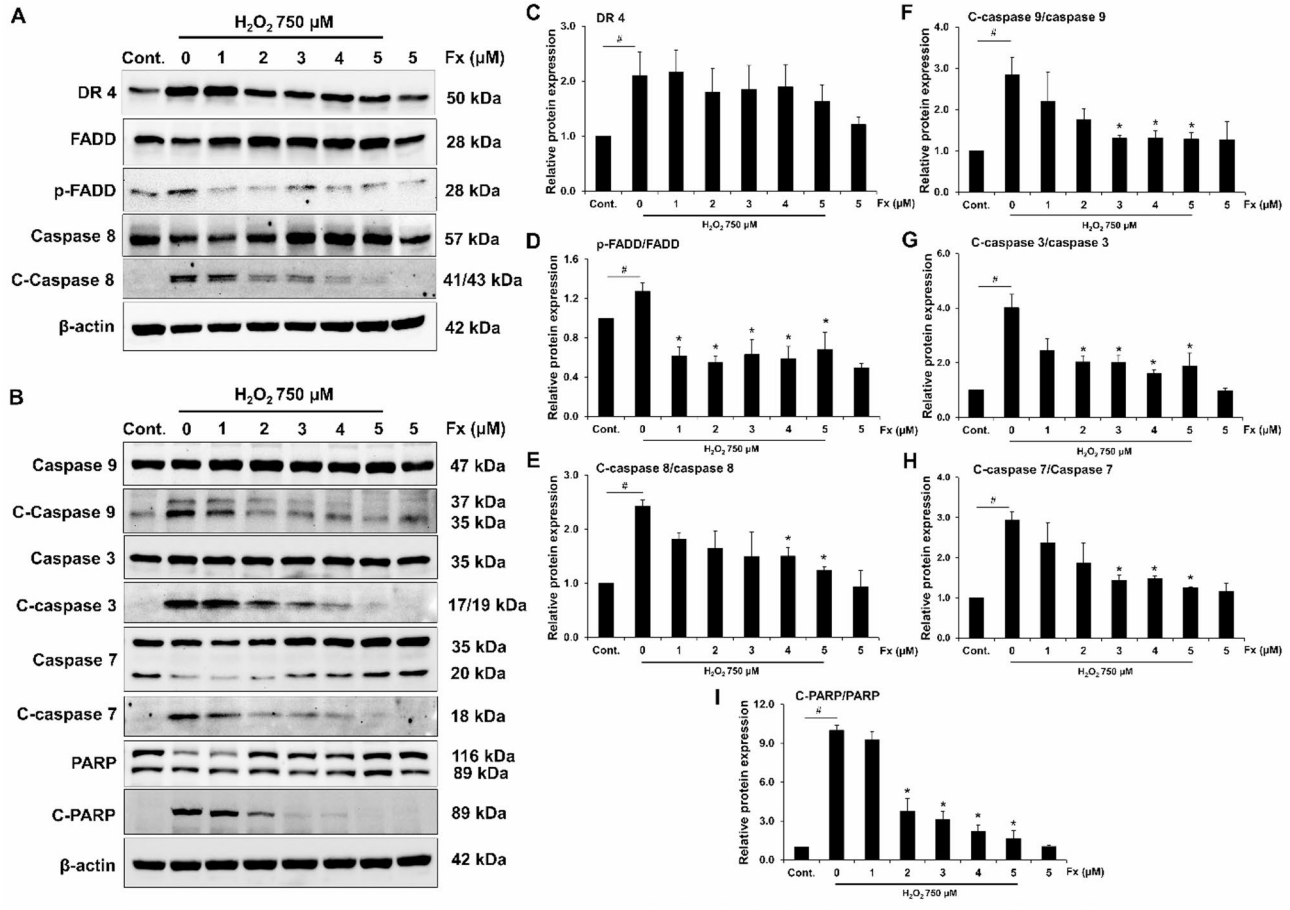

Fig. 4 Effects of fucoxanthin on proteins related to the extrinsic and intrinsic apoptotic pathway in H_2O_2-treated PL-MSCs. **A** Western blot analysis demonstrated DR4, p-FADD/FADD, and cleaved caspase 8/caspase 8 expression levels. **B** Western blot analysis demonstrated the expression levels of cleaved caspase 9/caspase 9, cleaved caspase-3/caspase 3, cleaved caspase 7/caspase 7, and cleaved PARP/PARP. The original blots are shown in Supplementary figures S2-S8. **C–I** The relative protein expression levels of DR4, p-FADD/FADD, cleaved caspase 8/caspase 8, cleaved caspase 9/caspase 9, cleaved caspase 3/caspase 3, cleaved caspase 7/caspase 7, and cleaved PARP/PARP in PL-MSCs after treatment with 750 μM H_2O_2 and fucoxanthin for 24 h. Data are presented as mean ± SEM, $n = 3$. A statistical significance of $^{\#}p \le 0.01$ indicates comparisons with control cultures of PL-MSCs in complete DMEM, while $^{*}p \le 0.05$ indicates comparisons with H_2O_2-treated PL-MSCs without fucoxanthin.

intrinsic apoptotic pathway in PL-MSCs under oxidative stress conditions by significantly decreasing the cleaved caspase 9/total caspase 9 protein ratio in a dose-dependent manner (Fig. 4B, F; Supplementary Fig. S5) (Table 1).

Consistent with these results, fucoxanthin also inhibited the activation of several executioner caspases in PL-MSCs under oxidative stress conditions, as demonstrated by a significant decrease in the ratios of cleaved caspase 3/total caspase 3, cleaved caspase 7/total caspase 7, and cleaved PARP/total PRAP proteins in H_2O_2-treated PL-MSCs compared to control (PL-MSCs treated with 750 µM H_2O_2) in a dose-dependent manner (Fig. 4B, G-I, Supplementary Fig. S6-S8). These findings suggest that fucoxanthin reduces PL-MSC apoptosis under oxidative stress conditions by decreasing the activation of proteins related to extrinsic and intrinsic apoptotic pathways.

Fucoxanthin increases PL-MSC viability under oxidative stress conditions by modulating the expression of genes involved in cell cycle regulation, DNA damage repair, ER stress response, P53-induced apoptosis

To study the effect of fucoxanthin on the global transcriptome of PL-MSCs under oxidative stress conditions, NanoString nCounter analysis was performed using the metabolic pathway panel to identify differentially expressed genes (DEGs). The results showed that fucoxanthin downregulated 23 genes mostly associated with apoptosis, unfolded protein response, the PI3K/Akt pathway and reactive oxygen response in the H_2O_2-treated PL-MSCs compared to controls (PL-MSCs treated with 750 µM H_2O_2) (Fig. 5A, B). Key downregulated genes included *UPP1* (fold change [FC] = – 1.59, $p = 0.002$), *PNP* (FC = – 1.44, $p = 0.029$), and *ERN1* (FC = – 1.39, $p = 0.000$), which are associated with ROS management and apoptosis (Fig. 5A, D, E; Table 2, Supplementary Tables 1 and 2). Conversely, 74 genes were upregulated, primarily involved in DNA repair and survival pathways. The top upregulated targets, such as *BUB1* (FC = 3.10, $p = 0.000$), *EME1* (FC = 2.99, $p = 0.001$), and *BUB1B* (FC = 2.81, $p = 0.000$), highlighted enhanced DNA damage repair and cell cycle regulation (Fig. 5A, D, E; Table 2 Supplementary Tables 1 and 2). These transcriptomic shifts suggest fucoxanthin mitigates oxidative stress by suppressing stress-response pathways while promoting genomic stability and survival.

The Venn diagram revealed distinct transcriptional responses between PL-MSCs subjected to oxidative stress (H_2O_2 treatment) and those co-treated with H_2O_2 and fucoxanthin. H_2O_2 treatment alone resulted in a downregulation of 75 genes associated with cell cycle progression and DNA repair pathways. In contrast, co-treatment with H_2O_2 and fucoxanthin led to an upregulation of 74 genes related to survival and DNA repair pathways. In particular, a significant overlap of genes whose expression was significantly altered between these two groups (59 genes, 65.6%) was observed. This result suggests that fucoxanthin reverses H_2O_2-induced suppression of critical pro-survival genes. In contrast to pro-survival genes, H_2O_2 upregulated 25 genes related to the stress response and the pro-apoptotic pathway. In which 14 of these genes (41.2%) were downregulated in PL-MSCs co-treated with H_2O_2 and fucoxanthin, indicated that fucoxanthin reverses H_2O_2-induced activation of stress response and pro-apoptotic pathway (Fig. 5C). Taken together, these findings suggest that fucoxanthin reduces oxidative damage by modulating the expression of several pro-survival, stress response and pro-apoptotic genes in PL-MSCs under oxidative stress conditions.

Gene Ontology (GO) analysis was performed to determine the biological functions of DEGs between H_2O_2-treated PL-MSCs and untreated control (Fig. 6A) and between PL-MSCs treated with H_2O_2 together with fucoxanthin and PL-MSCs treated with H_2O_2 alone (Fig. 6B). The results show that H_2O_2 treatment downregulated the expression of genes involved in the cell cycle regulation, DNA metabolism, DNA damage repair, and chromosomal organization, while upregulating the expression of

Table 1 List of primers used for qRT-PCR

Gene	Forward primer	Reserve primer	Product size (bp)
CASP3	5′-GAGGCGGTTGTGGAAGTTAA-3′	5′-GGATGCCGTCTAGAGTCCTA-3′	252
CASP8	5′-GTGCCCAAATCAACAAGAGC-3′	5′-ATCAGACAGTATCCCCGAGG-3′	222
APAF-1	5′-CTTCTTCCAGTGTAAGGACAGT-3′	5′-CAGCCTGCCATTCCATGTAT-3′	157
CYC C	5′-GGGTGATGTTGAGAAAGGCA-3′	5′-TTGTTCTTATTGGCGGCTGT-3′	164
BID	5′-CTTCTTCCAGTGTAAGGACAGT-3′	5′-CAGCCTGCCATTCCATGTAT-3′	116
BAD	5′-TGAGTGACGAGTTTGTGGAC-3′	5′-GTGGAGTTTCGGGATGTGG-3′	184
BAX	5′-CAGGGTTTCATCCAGGATCG-3′	5′-AGAAAACATGTCAGCTGCCA-3′	157
FADD	5′-ACACCAAGATCGACAGCATC-3′	5′-ATGCGTCTGAGTTCCATGAC-3′	240
TNFRSF10A	5′-TCAGCTGCAACCATCAAACT-3′	5′-ACTCTCCCAAAGGGCTATGT-3′	73
TNFRSF10B	5′-TTGAGGACCACTTGTTGAGC-3′	5′-CTTCCAGTACCGGTCATGTG-3′	186
BCL-2	5′-GGATTCCTGCGGATTGACAT-3′	5′-GGCAACGATCCCATCAATCT-3′	156
BIRC5	5′-GCCATTAACCGCCAGATTTG-3′	5′-AGAAGAAACACTGGGCCAAG-3′	89
GAPDH	5′-CAATGACCCCTTCATTGACC-3′	5′-TTGATTTTGGAGGGATCTCG-3′	158

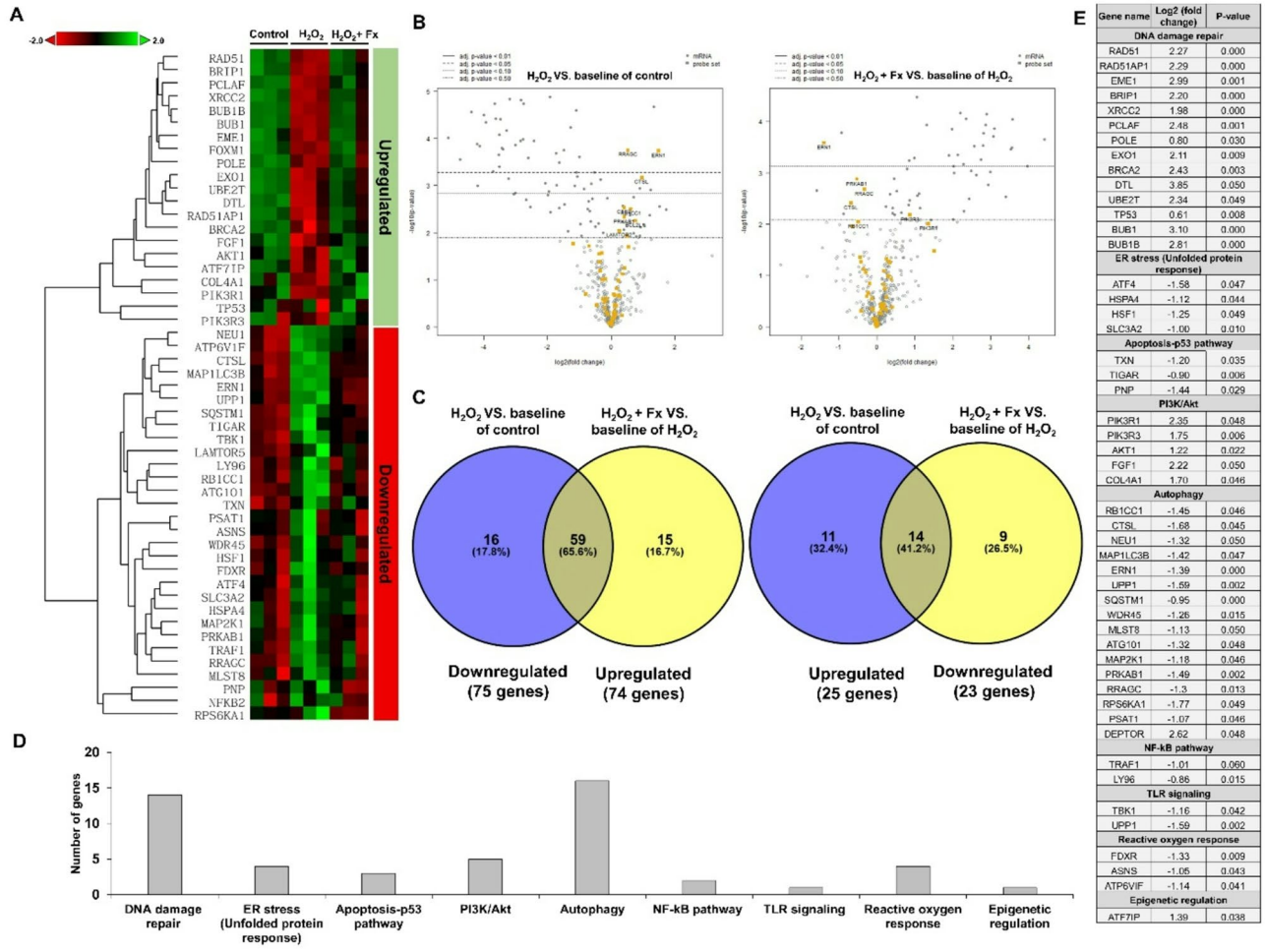

E

Gene name	Log2 (fold change)	P-value
DNA damage repair		
RAD51	2.27	0.000
RAD51AP1	2.29	0.000
EME1	2.99	0.001
BRIP1	2.20	0.000
XRCC2	1.98	0.000
PCLAF	2.48	0.001
POLE	0.80	0.030
EXO1	2.11	0.009
BRCA2	2.43	0.003
DTL	3.85	0.050
UBE2T	2.34	0.049
TP53	0.61	0.008
BUB1	3.10	0.000
BUB1B	2.81	0.000
ER stress (Unfolded protein response)		
ATF4	-1.58	0.047
HSPA4	-1.12	0.044
HSF1	-1.25	0.049
SLC3A2	-1.00	0.010
Apoptosis-p53 pathway		
TXN	-1.20	0.035
TIGAR	-0.90	0.006
PNP	-1.44	0.029
PI3K/Akt		
PIK3R1	2.35	0.048
PIK3R3	1.75	0.006
AKT1	1.22	0.022
FGF1	2.22	0.050
COL4A1	1.70	0.046
Autophagy		
RB1CC1	-1.45	0.046
CTSL	-1.68	0.045
NEU1	-1.32	0.050
MAP1LC3B	-1.42	0.047
ERN1	-1.39	0.000
UPP1	-1.59	0.002
SQSTM1	-0.95	0.000
WDR45	-1.26	0.015
MLST8	-1.13	0.050
ATG101	-1.32	0.048
MAP2K1	-1.18	0.046
PRKAB1	-1.49	0.002
RRAGC	-1.3	0.013
RPS6KA1	-1.77	0.049
PSAT1	-1.07	0.046
DEPTOR	2.62	0.048
NF-kB pathway		
TRAF1	-1.01	0.060
LY96	-0.86	0.015
TLR signaling		
TBK1	-1.16	0.042
UPP1	-1.59	0.002
Reactive oxygen response		
FDXR	-1.33	0.009
ASNS	-1.05	0.043
ATP6VIF	-1.14	0.041
Epigenetic regulation		
ATF7IP	1.39	0.038

Fig. 5 NanoString analysis of differential gene expressions related to apoptosis and its associated pathways in PL-MSCs subjected to oxidative stress. **A** A heatmap displays the differentially expressed genes (DEGs) in PL-MSCs treated with 750 μM H_2O_2 and PL-MSCs treated with 750 μM H_2O_2 and 5 μM fucoxanthin. **B** Volcano plots highlight individual differentially expressed genes. The X-axis represents -log10 (p-value) while the Y-axis represents the log2 fold change between each pair of treatment groups. **C** A Venn diagram of DEGs shows the intersection of up-regulated and down-regulated genes in PL-MSCs treated with 750 μM H_2O_2 and 5 μM fucoxanthin, compared to those treated with 750 μM H_2O_2. **D** A bar plot representative of genes in PL-MSCs treated with 750 μM H_2O_2 and 5 μM fucoxanthin compared to those treated with 750 μM H_2O_2. The Y-axis represents the number of genes, while the X-axis represents the signaling pathway/function involved with apoptosis and its associated pathways. **E** Fold change and statistical significance (p-value) in gene expression of fucoxanthin-treated PL-MSCs compared to untreated PL-MSCs under oxidative stress.

genes involved in the oxidative stress response and apoptosis in PL-MSCs (Fig. 6A).

Consistent with its survival-promoting effect on PL-MSCs under oxidative stress conditions, fucoxanthin increases the expression levels of genes involved in the cell cycle regulation, DNA damage repair, cytokine signaling, nucleotide synthesis, PI3K/mTOR pathway and AMPK pathways in PL-MSCs that were initially downregulated by the H_2O_2 treatment, while downregulating the expression levels of genes involved in apoptosis, and ER stress response (Fig. 6B).

Consistent with the GO analysis, the analyses of the Kyoto Encyclopedia of Genes and Genomes (KEGG) pathway also showed that H_2O_2 treatment significantly downregulated the expression levels of genes involved in the regulation of the cell cycle, DNA damage repair, cytokine signaling, nucleotide synthesis, PI3K/mTOR pathway and AMPK pathways in PL-MSCs (Fig. 7A) and that treatment with fucoxanthin increased the expression levels of genes involved in the regulation of the cell cycle, DNA damage repair, cytokine signaling, nucleotide synthesis, PI3K/mTOR pathway and AMPK pathways in PL-MSCs that were initially downregulated by H_2O_2 treatment (Fig. 7B).

The PPI network analysis further showed that the top 20 downregulated DEGs in H_2O_2-treated PL-MSCs have 139 interaction partners, which were enriched in pathways related to DNA replication initiation, PI3K/Akt and DNA damage repair (Fig. 8A), while the top 20 upregulated DEGs in H_2O_2-treated PL-MSCs have 68

Table 2 Fold change of gene expression in fucoxanthin-treated PL-MSCs compared to untreated PL-MSCs under oxidative stress conditions

Upregulated Genes	Function/Pathway	Fold change	*P* value
BUB1	BUB1 mitotic checkpoint serine/threonine kinase	3.10	0.000
EME1	Essential meiotic structure-specific endonuclease 1	2.99	0.001
BUB1B	BUB1 Mitotic Checkpoint Serine/Threonine Kinase B	2.81	0.000
PCLAF	PCNA Clamp Associated Factor	2.56	0.000
BRCA2	BRCA2 DNA Repair Associated	2.43	0.003
RAD51AP1	RAD51 Associated Protein 1	2.29	0.000
RAD51	DNA repair protein RAD51 homolog 1	2.27	0.006
BRIP1	BRCA1 Interacting DNA Helicase 1	2.20	0.000
EXO1	Exonuclease 1	2.11	0.009
XRCC2	X-Ray Repair Cross-Complementing 2	1.98	0.000
Downregulated Genes	**Function/Pathway**	**Fold change**	***P* value**
UPP1	Uridine phosphorylase 1	-1.59	0.002
PNP	Purine Nucleoside Phosphorylase	-1.44	0.029
ERN1	Endoplasmic reticulum to nucleus signaling 1	-1.39	0.000
FDXR	Ferredoxin Reductase	-1.33	0.009
PSAT1	Phosphoserine Aminotransferase 1	-1.07	0.046
ASNS	Asparagine Synthetase	-1.05	0.043
SLC3A2	Solute carrier family 3 member 2	-1.00	0.010
SQSTM1	Sequestosome 1	-0.95	0.000
TIGAR	TP53-inducible glycolysis and apoptosis regulator	-0.90	0.006
LY96	Lymphocyte Antigen 96	-0.86	0.015

interaction partners enriched in oxygen stress response and apoptosis pathways (Fig. 8B). Consistent its positive effect on PL-MSC survival, fucoxanthin upregulated genes enriched in pathways related to DNA replication initiation, PI3K/Akt activation and DNA damage repair (Fig. 8C) and downregulated genes enriched in pathways related to ROS detoxification and apoptosis (Fig. 8D). The transcription factor (TF) analysis showed that the p53 (TP53, $p < 0.0001$), E2F transcription factor 1 (E2F1, $p < 0.0001$), and E2F transcription factor 4 (E2F4, $p < 0.0001$) were significantly associated with oxidative stress responses in PL-MSCs (Fig. 8E–F). These TFs, whose expressions were enriched in both (1) H_2O_2-treated PL-MSCs compared to untreated controls and (2) H_2O_2 and fucoxanthin-treated PL-MSCs compared to the H_2O_2 only group, play an important role in the regulation of cell cycle progression, DNA replication, and cell growth (Table 3). The consistent prominence of tumor suppressor TP53 and cell cycle regulators, E2F1/E2F4, underscores their important role in balancing stress adaptation and survival pathways in PL-MSCs under oxidative stress conditions.

Taken together, these results suggest that fucoxanthin increases PL-MSC viability under oxidative stress conditions by modulating the expression of various genes involved in cell cycle regulation, DNA damage repair, ER stress response, p53-induced apoptosis.

Discussion

Human mesenchymal stem cells hold significant promise in regenerative medicine due to their ability to home in specific tissues and release various beneficial factors to reduce inflammation and promote tissue repair [20–22]. Although BM-MSCs are the most extensively studied [23, 24], several limitations hinder their clinical uses, especially limited availability, invasive harvesting procedures and a decrease in proliferation and differentiation capacity after culture expansion [25, 26]. Therefore, alternative sources of MSC, such as PL-MSCs, which have greater expansion potential than BM-MSCs and are easier to obtain by non-invasive procedures [27–29], are considered more suitable for research and clinical use [30, 31]. Consistent with previous reports, the characteristics of PL-MSCs established in this study met all the criteria for defining mesenchymal stromal cells recommended by the International Society for Cell & Gene Therapy [32], including adherence, expression of MSC surface markers, and trilineage differentiation capacity.

Regardless of the source of MSCs, previous studies showed that the viability of MSCs at the transplanted sites is compromised by oxidative stress and hypoxic microenvironment in targeted tissues [5, 33, 34]. Therefore, it is essential to develop strategies to increase MSC survival under oxidative stress conditions to improve their therapeutic potential for regenerative medicine applications.

The unique chemical structure of fucoxanthin, including its allenic bond and oxygen-rich functional groups (e.g., epoxides, hydroxyl groups), enables potent free radical scavenging, directly neutralizing ROS generated under oxidative stress [35]. This aligns with our data showing reduced intracellular ROS levels in H_2O_2-treated PL-MSCs co-treated with fucoxanthin. Recent studies showed that co-treatment and pre-treatment with the algal carotenoid fucoxanthin promotes cell survival under oxidative stress by reducing intracellular ROS and increasing the expression and activity of antioxidant enzymes in human hepatic cell lines [36], human retinal epithelial cells [12, 13], and human BM-MSCs [37]. Consistent with this, our previous study showed that fucoxanthin also increases the viability of PL-MSCs under oxidative stress conditions by increasing the activity of the antioxidant enzymes SOD and GSH, reducing intracellular ROS production, and activating PI3K/Akt/Nrf-2

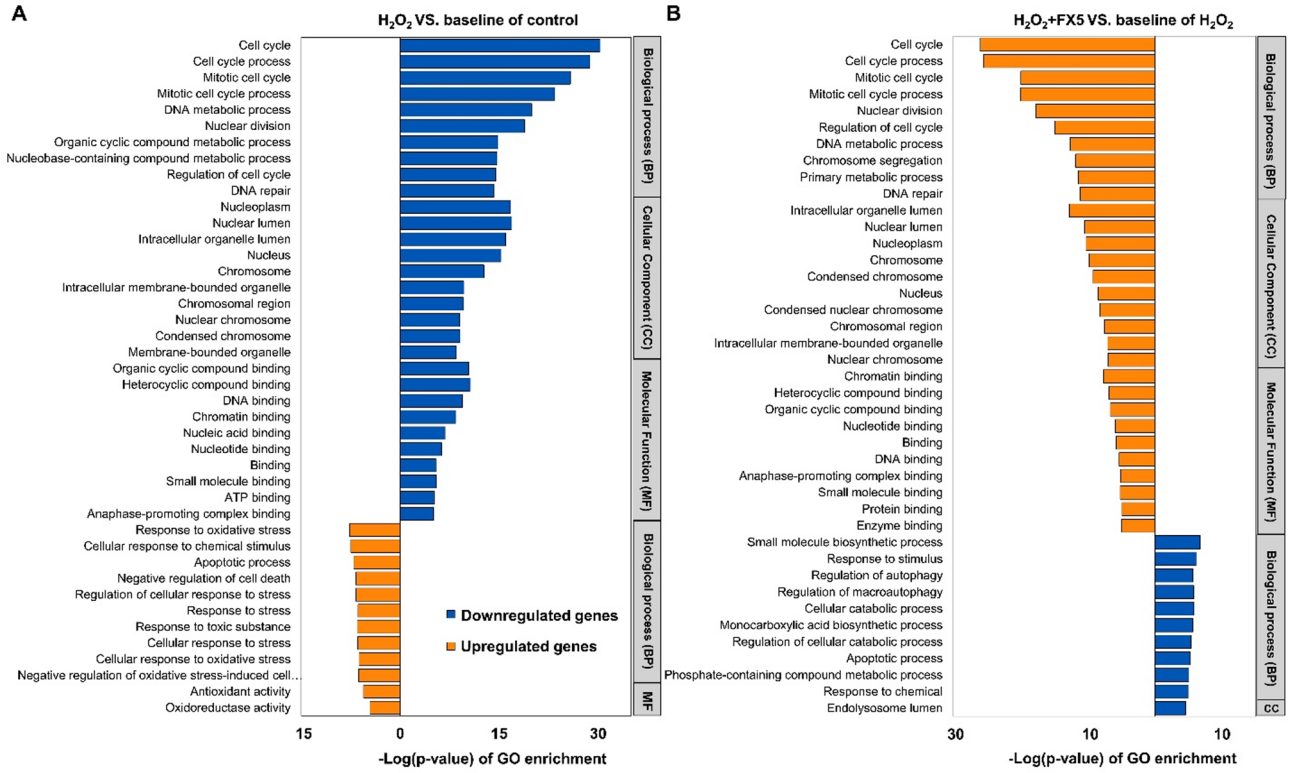

Fig. 6 The Gene Ontology (GO) enrichment analysis for the top 10 ranked GO enrichments across three functional classifications: Biological Process, Cellular Component, and Molecular Function, based on the DEGs. **A** The GO term was significantly associated with DEGs in PL-MSCs treated with 750 μM H_2O_2, compared to the untreated control. **B** The GO term for PL-MSCs treated with both 750 μM H_2O_2 and 5 μM fucoxanthin, relative to the baseline of H_2O_2-treated PL-MSCs. The X-axis represents -Log(p-value) of GO enrichment, which indicates the number of genes involved. The Y-axis represents the GO terms. Significantly upregulated DEGs are shown in orange, while significantly downregulated DEGs are shown in blue

signaling pathways [15]. Moreover, high-throughput analysis revealed a dual role of fucoxanthin, which upregulates the survival pathway and downregulates apoptosis. Enhanced expression of DNA repair (*BUB1*, *RAD51*) and cell cycle genes (*cyclin D1*) promotes proliferation and genomic stability. Suppression of stress-response genes (*UPP1*, *ERN1*) reduces programmed cell death [15]. By concurrently scavenging ROS and activating repair/survival pathways, fucoxanthin creates a protective feedback loop. This dual action prevents oxidative damage from overwhelming cellular defenses, as evidenced by full viability restoration at 24 h and partial recovery at 48 h. Therefore, fucoxanthin enhances MSC viability through ROS neutralization, antioxidant pathway activation, and transcriptomic shifts favoring survival over apoptosis.

In this study, we focused on 24-h and 48-h time points to assess acute responses to oxidative stress and fucoxanthin intervention. The selection was guided by their clinical and mechanistic relevance to MSC therapies. In clinical settings, such as post-transplantation ischemia-reperfusion injury, MSCs encounter transient oxidative stress within these acute windows, making our experimental timeline reflective of real-world therapeutic scenarios. Furthermore, these timeframes provide mechanistic clarity: the 24-h period captures early apoptotic signaling and immediate stress responses, while the 48-h interval reveals cumulative damage and progressive repair processes, offering a holistic view of the cytoprotective effects of fucoxanthin. Our findings demonstrate that fucoxanthin restores PL-MSC viability in a time- and dose-dependent manner. At 24 h, 5 μM fucoxanthin fully rescued viability (101.82% ± 3.71), aligning with its potent antioxidant and anti-apoptotic properties observed in prior studies. By contrast, viability restoration at 48 h was partial (82.09% ± 4.47), suggesting that prolonged oxidative stress overwhelms reparative mechanisms despite treatment with fucoxanthin. This diminishing efficacy under chronic stress underscores the importance of early therapeutic administration in clinical contexts. The differential recovery rates may stem from the dual role of fucoxanthin, scavenging reactive oxygen species (ROS) to mitigate acute damage while simultaneously activating survival pathways like PI3K/Akt/Nrf-2, which may lose efficacy as oxidative insults persist [15].

While this study provides critical insights into the acute protective effects of fucoxanthin, longer-term observations (e.g., 72–96 h) were omitted to avoid confounding factors such as nutrient depletion or spontaneous

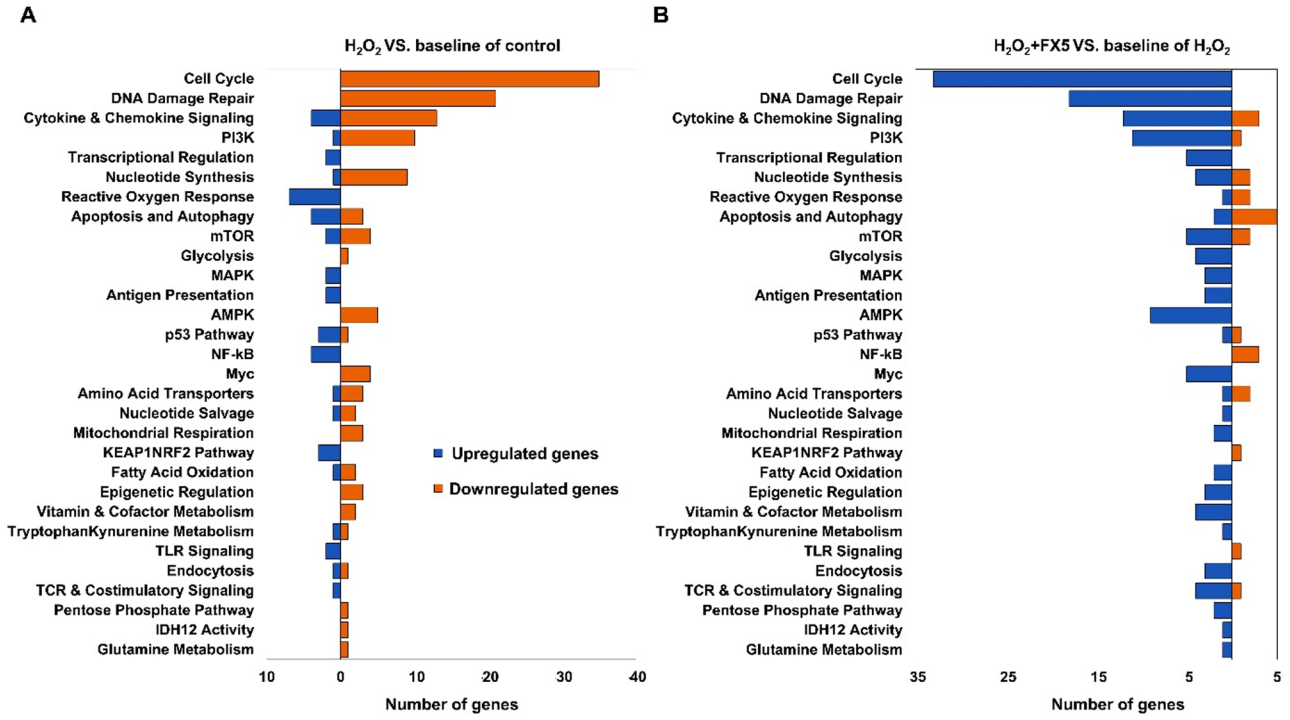

Fig. 7 The KEGG analysis of PL-MSCs under oxidative stress conditions was conducted using the Shiny GO web application. **A** KEGG term for significant DEGs in PL-MSCs treated with 750 μM H_2O_2 compared to the untreated control. **B** KEGG term in PL-MSCs treated with 750 μM H_2O_2 and 5 μM fucoxanthin, compared to the baseline H_2O_2-treated PL-MSCs. The X-axis represents the number of genes, while the Y-axis represents the KEGG pathway term. Significantly upregulated DEGs are shown in blue, while downregulated DEGs are displayed in orange

differentiation in monolayer cultures. Future work employing 3D culture systems or in vivo models could better replicate the dynamic microenvironments MSCs encounter post-transplantation, enabling assessment of chronic stress adaptation and functional integration. Additionally, coupling viability assays with real-time metabolic profiling could clarify how fucoxanthin modulates energy utilization under oxidative duress. These findings position fucoxanthin as a promising adjuvant for enhancing MSC resilience in oxidative environments, particularly in acute settings. By bridging mechanistic insights with clinically relevant timeframes, this work lays a foundation for optimizing MSC-based therapies in regenerative medicine.

Additionally, we showed that fucoxanthin mitigated PL-MSC apoptosis under oxidative stress conditions by decreasing the expression and activation of pro-apoptotic proteins, including FADD, caspase 8, caspase 9, caspase 7, caspase 3, PARP, Bid, Bad, and Bax, while increasing the expression of anti-apoptotic proteins Bcl-2 and Survivin (Fig. 9). The results are consistent with previous studies showing that fucoxanthin down-regulated pro-apoptotic proteins Bax, caspase 9, caspase 3, and p53, and up-regulated anti-apoptotic proteins, Bcl-2, in human keratinocytes [10], human renal proximal tubular epithelial HK-2 cells [38] and human BM-MSCs [37]. Furthermore, fucoxanthin reduced ER stress and prevented amyloid β protein fragment-induced apoptosis in rat glial cells by reducing the levels of proteins associated with ER stress and apoptosis, such as CCAAT/enhancer-binding protein homologous protein (CHOP), caspase 12, caspase 3 and Bax [39].

In addition to its inhibitory effect on pro-apoptotic genes and proteins, our results showed that fucoxanthin also increased the expression levels of genes involved in the cell cycle regulation, DNA damage repair, cytokine signaling, nucleotide synthesis, PI3K/mTOR pathway and AMPK pathways in PL-MSCs that were down-regulated under oxidative stress condition. Furthermore, fucoxanthin also reduced the expression levels of genes involved in apoptosis, and the ER stress response in these PL-MSCs. This is consistent with previous studies showing that fucoxanthin increases cell viability by protecting cells against oxidative damage and decreasing the expression of genes associated with ER stress and apoptosis, including *ERN1* (also known as *IRE1*), *ATF4*, *HSF1* and *HSPA4* [40–42]. In addition, our results suggest that fucoxanthin decreases PL-MSC apoptosis under oxidative stress conditions by downregulating genes, such as *UPP1*, *SQSTM1*, *CTSL* and *PRKAB1*, as shown through NanoString pathway analysis, which is consistent with previous studies showing that these genes can trigger apoptosis under certain circumstances through the

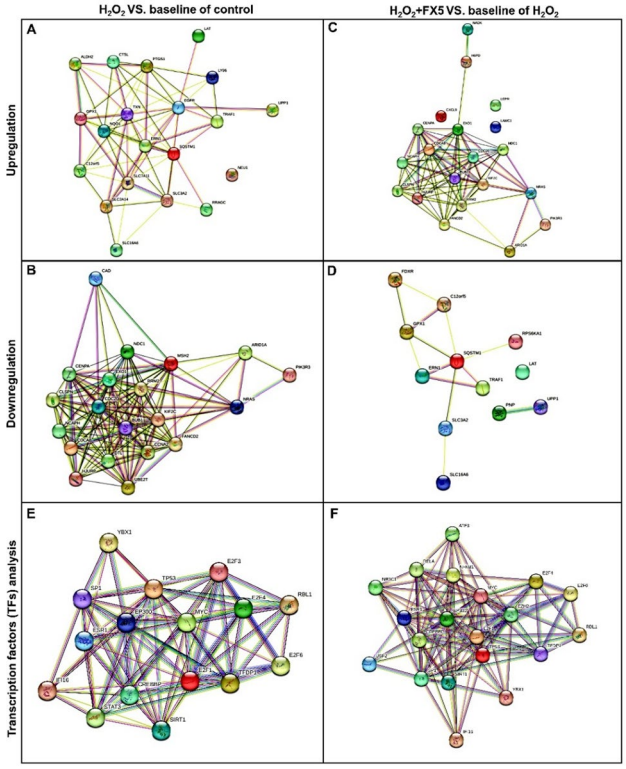

Fig. 8 Protein-protein interaction (PPI) networks were analyzed using STRING to identify functional clusters of differentially expressed genes (DEGs). **A** Upregulated protein cluster in PL-MSCs treated with 750 μM H_2O_2 vs. untreated controls, linked to oxidative stress adaptation. **B** Downregulated protein cluster in H_2O_2-treated PL-MSCs vs. controls, associated with suppressed metabolic pathways. **C** Upregulated protein cluster in H_2O_2 and 5 μM fucoxanthin-treated PL-MSCs vs. H_2O_2-only, enriched in DNA repair and survival pathways. **D** Downregulated protein cluster in H_2O_2 and fucoxanthin vs. H_2O_2-only, highlighting reduced apoptosis signaling. **E** Predicted transcription factors (TFs) for DEGs in H_2O_2-treated PL-MSCs vs. controls, dominated by stress-responsive regulators (e.g., TP53, E2F1). **F** TF network for DEGs in H_2O_2 and fucoxanthin vs. H_2O_2-only, revealing fucoxanthin-driven modulation of cell cycle and survival TFs

Table 3 Top 10 predicted key transcription factors (TFs) in PL-MSCs treated with 750 μM H_2O_2 compared to those treated with 750 μM H_2O_2 and 5 μM Fucoxanthin

Key TFs	Role/Associated Pathway	*P* value	FDR
PL-MSCs treated with 750 μM H_2O_2 vs. untreated control			
TP53	Tumor protein p53	1.82e-13	9.66e-12
E2F1	E2F transcription factor 1	1.25e-10	3.32e-09
JUN	Jun proto-oncogene	9.61e-08	1.63e-06
TFDP1	Transcription factor Dp-1	1.52e-07	1.63e-06
ESR1	Estrogen receptor 1	1.53e-07	1.63e-06
CREBBP	CREB binding protein	1.84e-07	1.63e-06
MYC	v-myc myelocytomatosis viral oncogene homolog	1.01e-06	7.67e-06
SP1	Sp1 transcription factor	1.23e-06	8.18e-06
STAT1	Signal transducer and activator of transcription 1, 91 kDa	5.53e-06	3.22e-05
E2F4	E2F transcription factor 4, p107/p130-binding	6.08e-06	3.22e-05
PL-MSCs treated with 750 μM H_2O_2 and 5 μM fucoxanthin vs. H_2O_2-treated PL-MSCs			
TP53	Tumor protein p53	2.08e-14	7.48e-13
E2F1	E2F transcription factor 1	2.35e-11	4.24e-10
E2F4	E2F transcription factor 4, p107/p130-binding	3.33e-06	4e-05
CREBBP	CREB binding protein	4.73e-06	4.25e-05
MYC	v-myc myelocytomatosis viral oncogene homolog	6.34e-06	4.57e-05
TFDP1	Transcription factor Dp-1	1.07e-05	6.43e-05
MEN1	Multiple endocrine neoplasia I	1.47e-05	7.55e-05
SP1	Sp1 transcription factor	5.6e-05	0.000252
EP300	E1A binding protein p300	0.000123	0.000493
CHD8	Chromodomain helicase DNA-binding protein 8	0.000204	0.000611

activation of caspase 8 and the depletion of endogenous apoptosis inhibitors [43–45].

The Venn diagram provided valuable information on the effect of fucoxanthin in reducing oxidative stress-induced transcriptional dysregulation in PL-MSCs. The substantial overlap of 59 genes (65.6%) whose expression was downregulated by H_2O_2 treatment but upregulated by co-treatment of H_2O_2 and fucoxanthin suggests that fucoxanthin effectively restores the expression of genes involved in cellular homeostasis, antioxidant, and DNA repair processes. This effect aligns with the unique chemical structure of fucoxanthin, characterized by its abundant allenic C-H bonds and oxygen-containing groups, which facilitates the ROS scavenging and the modulation of redox signaling pathways. Furthermore, the partial suppression of H_2O_2-induced upregulation of stress-response genes (14 genes, 41.2%) in the co-treatment group suggests that fucoxanthin also reverses H_2O_2-induced activation of stress response and pro-apoptotic pathway. This finding is consistent with the fucoxanthin capacity to activate pro-survival signaling pathways, such as the PI3K/Akt/Nrf-2 axis observed in previous research [15].

Our findings are also consistent with previous studies that demonstrate the cytoprotective effects of fucoxanthin on hepatic and retinal cells by increasing the activity of antioxidant enzymes, such as superoxide dismutase (SOD) and glutathione peroxidase (GSH), and reducing stress-induced apoptosis in these cells [12, 13, 36]. The increased expression levels of *BUB1*, *RAD51*, and other DNA repair genes further support the role of fucoxanthin in promoting DNA repair and genomic stability under oxidative stress. This is crucial to improve the viability of MSCs during therapeutic applications [38]. However, it is essential to note that the restoration of H_2O_2-induced gene dysregulation, such as those related to apoptotic signaling, by fucoxanthin treatment is incomplete. This underscores the complexity of oxidative damage that might require a combination treatment to further

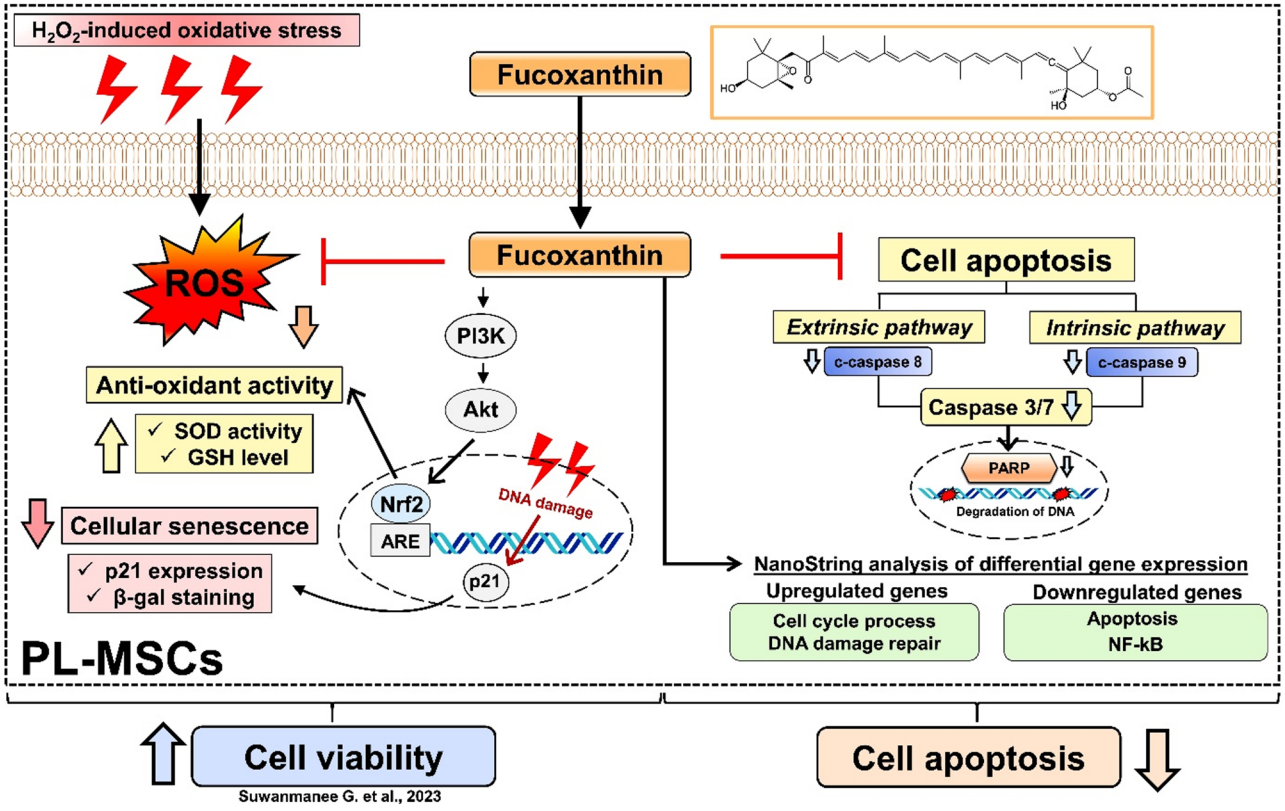

Fig. 9 A schematic diagram illustrates how fucoxanthin mitigates oxidative stress and enhances PL-MSC survival

enhance the viability of MSCs under severe oxidative stress conditions.

The results suggest that the TP53 and E2F1/2 networks could corroborate the ability of fucoxanthin to activate the PI3K/Akt/Nrf-2 pathways, enhance DNA repair by upregulating the expression of *BUB1* and *RAD51* genes, and suppress the expression of the pro-apoptotic *CASP8* gene, to increase PL-MSC viability by balancing stress adaptation and survival. However, future research is required to investigate the long-term effect of fucoxanthin on MSC properties, using an in vivo model to confirm its therapeutic efficacy. Furthermore, additional proteomic and metabolomic analyzes should be performed to further elucidate the molecular mechanisms that contribute to the cytoprotective effects of fucoxanthin.

Conclusions

This study provides compelling evidence that fucoxanthin protects PL-MSCs against oxidative stress-induced apoptosis by modulating the expression of many genes involved in cell cycle regulation, DNA damage repair, ER stress response, p53-induced apoptosis in these cells (Fig. 9). We believe that fucoxanthin could be used in combination with other agents to increase the therapeutic potential of MSCs by improving their viability in the oxidative stress microenvironment of the target tissues.

Abbreviations

APAF-1	Apoptotic protease activating factor 1
BAD	BCL-2 associated agonist of cell death
BAX	BCL-2–associated X
BCL-2	B-cell lymphoma 2
BID	BH3 interacting-domain death agonist
BIRC5	Survivin
BM-MSCs	Bone marrow-derived mesenchymal stem cells
CASP3	Caspase 3
CASP8	Caspase 8
cDNA	Complementary deoxyribonucleic acid
CHOP	CCAAT/enhancer-binding protein homologous protein
CO_2	Carbon dioxide
CYC C	Cytochrome c
DEGs	Differential expression of genes
DMEM	Dulbecco's modified Eagle's medium
DNA	Deoxyribonucleic acid
ECL	Enhanced chemiluminescence
FADD	Fas-associated death domain
FBS	Fetal bovine serum
FITC	Fluorescein isothiocyanate
GAPDH	Glyceraldehyde-3-phosphate dehydrogenase
GO	Gene ontology
H_2O_2	Hydrogen peroxide
HLA-DR	Human leukocyte antigen – DR isotype
hMSCs	Human mesenchymal stem cells
HRP	Horseradish peroxidase
KEGG	Kyoto Encyclopedia of Genes and Genomes
OD	Optical density

PBS	Phosphate-buffered saline
PE	Phycoerythrin
p-FADD	Phosphorylated Fas-associated death domain
PI3K	Phosphoinositide 3-kinase
PL-MSCs	Placenta-derived mesenchymal stem cells
PPI	Protein-protein interaction
qRT-PCR	Quantitative reverse transcription polymerase chain reaction
ROS	Reactive oxygen species
SEM	Standard error of the mean
tBid	Truncated BH3-interacting domain death agonist
TBST	Tris-buffered saline with Tween 20 detergent
TNFRSF10A	Tumor necrosis factor receptor superfamily member 10A
TNFRSF10B	Tumor necrosis factor receptor superfamily member 10B

Supplementary Information

The online version contains supplementary material available at https://doi.org/10.1186/s13287-025-04629-3.

Supplementary Material 1

Supplementary Material 2

Supplementary Material 3

Acknowledgements
The authors would like to express their gratitude to the staff of the delivery room at Thammasat University Hospital for their assistance in collecting the specimens. They also extend their appreciation to all research participants who generously donated tissues for this study. Additionally, the authors declare that they did not use any AI-generated content in this manuscript.

Author contributions
G.S. conducted the experiments and drafted the manuscript. C.T. contributed to the data interpretation. D.G., I.M. P.K. also assisted with data interpretation and revised the manuscript. L.P. was involved in conceptualization, provided resources, supervised the work, contributed to data interpretation and revised the manuscript. S.M. contributed to conceptualization, study design, resources, funding, supervision, data analysis and interpretation, and was responsible for drafting and completing the manuscript. All authors read and approved the final manuscript.

Funding
This work was supported by the Thailand Science Research and Innovation Fundamental Fund for the fiscal year 2024, Thammasat University (Grant No. TUFF 52/2567), and the Royal Golden Jubilee (RGJ) Ph.D. program (Grant No. NRCT5-RGJ63008-098) through the National Research Council of Thailand (NRCT) and the Thailand Research Fund (TRF). Additionally, support was provided by the Faculty of Medicine, Thammasat University and the Center of Excellence in Stem Cell Research and Innovation at Thammasat University. The funding body had no role in the design of this study, the collection, analysis, or interpretation of the data, nor in the writing of the manuscript.

Data availability
The data that support the findings of this study are available in the supplementary material of this article.

Declarations

Ethics approval and consent to participate
All experimental procedures were conducted under the Declaration of Helsinki and the Belmont Report. This study received approval from the Human Research Ethics Committee of Thammasat University (Medicine) under the title "Approval title: The effects of fucoxanthin on the proliferation and osteogenic differentiation of human mesenchymal stem cells." (Approval number: 024/2021, Date of approval: February 4, 2021). All samples were obtained from donors who provided written informed consent.

Consent for publication
Not applicable.

Competing Interests
The authors declare that they have no competing interests.

Author details
[1]Division of Cell Biology, Department of Preclinical Sciences, Faculty of Medicine, Thammasat University, Pathumthani 12120, Thailand
[2]Center of Excellence in Stem Cell Research and Innovation, Thammasat University, Pathumthani 12120, Thailand
[3]Department of Biology, Faculty of Arts and Sciences, Edge Hill University, BioSciences Building, St Helens Road, Ormskirk L39 4QP, UK
[4]Department of Life Sciences, Faculty of Science and Engineering, Manchester Metropolitan University, Dalton Rm 5.35, Chester Street, Manchester M1 5GD , UK

Received: 24 March 2025 / Accepted: 25 August 2025
Published online: 25 September 2025

References

1. Le Blanc K, et al. Treatment of severe acute graft-versus-host disease with third party haploidentical mesenchymal stem cells. Lancet. 2004;363(9419):1439–41.
2. Huang Y, Wu Q, Tam PKH. Immunomodulatory mechanisms of mesenchymal stem cells and their potential clinical applications. Int J Mol Sci, 2022. 23(17).
3. Li L, et al. How to improve the survival of transplanted mesenchymal stem cell in ischemic heart?? Stem Cells Int. 2016;2016:p9682757.
4. Schrepfer S, et al. Stem cell transplantation: the lung barrier. Transpl Proc. 2007;39(2):573–6.
5. Amiri F, Jahanian-Najafabadi A, Roudkenar MH. Vitro augmentation of mesenchymal stem cells viability in stressful microenvironments: in vitro augmentation of mesenchymal stem cells viability. Cell Stress Chaperones. 2015;20(2):237–51.
6. Jomova K, et al. Reactive oxygen species, toxicity, oxidative stress, and antioxidants: chronic diseases and aging. Arch Toxicol. 2023;97(10):2499–574.
7. Maeda H. Nutraceutical effects of Fucoxanthin for obesity and diabetes therapy: a review. J Oleo Sci. 2015;64(2):125–32.
8. Ahmed SA et al. Anticancer effects of Fucoxanthin through cell cycle arrest, apoptosis induction, angiogenesis inhibition, and autophagy modulation. Int J Mol Sci, 2022. 23(24).
9. Guan B et al. Advances in Fucoxanthin research for the prevention and treatment of Inflammation-Related diseases. Nutrients, 2022. 14(22).
10. Zheng J, et al. Fucoxanthin protects cultured human keratinocytes against oxidative stress by blocking free radicals and inhibiting apoptosis. Biomol Ther (Seoul). 2013;21(4):270–6.
11. Zheng J, et al. Fucoxanthin enhances the level of reduced glutathione via the Nrf2-mediated pathway in human keratinocytes. Mar Drugs. 2014;12(7):4214–30.
12. Chen SJ et al. Cytoprotective potential of Fucoxanthin in oxidative Stress-Induced Age-Related macular degeneration and retinal pigment epithelial cell senescence in vivo and in vitro. Mar Drugs, 2021. 19(2).
13. Chiang YF et al. Protective effects of Fucoxanthin on high Glucose- and 4-Hydroxynonenal (4-HNE)-Induced injury in human retinal pigment epithelial cells. Antioxid (Basel), 2020. 9(12).
14. Yu J, et al. Fucoxanthin prevents H(2)O(2)-induced neuronal apoptosis via concurrently activating the PI3-K/Akt cascade and inhibiting the ERK pathway. Food Nutr Res. 2017;61(1):1304678.
15. Suwanmanee G, et al. Fucoxanthin diminishes oxidative stress damage in human placenta-derived mesenchymal stem cells through the PI3K/Akt/Nrf-2 pathway. Sci Rep. 2023;13(1):22974.
16. Talwadekar MD, Kale VP, Limaye LS. Placenta-derived mesenchymal stem cells possess better immunoregulatory properties compared to their cord-derived counterparts-a paired sample study. Sci Rep. 2015;5:15784.
17. Manochantr S, et al. Immunosuppressive properties of mesenchymal stromal cells derived from amnion, placenta, wharton's jelly and umbilical cord. Intern Med J. 2013;43(4):430–9.
18. Ge SX, Jung D, Yao R. ShinyGO: a graphical gene-set enrichment tool for animals and plants. Bioinformatics. 2019;36(8):2628–9.
19. Han H, et al. TRRUST v2: an expanded reference database of human and mouse transcriptional regulatory interactions. Nucleic Acids Res. 2018;46(D1):D380–6.

20. Cooper K, Viswanathan C. Establishment of a mesenchymal stem cell bank. Stem Cells Int. 2011;2011:905621.
21. Margiana R, et al. Clinical application of mesenchymal stem cell in regenerative medicine: a narrative review. Stem Cell Res Ther. 2022;13(1):366.
22. Satija NK, et al. Mesenchymal stem cell-based therapy: a new paradigm in regenerative medicine. J Cell Mol Med. 2009;13(11–12):4385–402.
23. Pittenger MF, et al. Multilineage potential of adult human mesenchymal stem cells. Science. 1999;284(5411):143–7.
24. Marquez-Curtis LA, et al. Mesenchymal stromal cells derived from various tissues: biological, clinical and cryopreservation aspects. Cryobiology. 2015;71(2):181–97.
25. Stenderup K, et al. Aging is associated with decreased maximal life span and accelerated senescence of bone marrow stromal cells. Bone. 2003;33(6):919–26.
26. Baker N, Boyette LB, Tuan RS. Characterization of bone marrow-derived mesenchymal stem cells in aging. Bone. 2015;70:37–47.
27. Li X, et al. Human placenta-derived adherent cells prevent bone loss, stimulate bone formation, and suppress growth of multiple myeloma in bone. Stem Cells. 2011;29(2):263–73.
28. Uccelli A, Moretta L, Pistoia V. Mesenchymal stem cells in health and disease. Nat Rev Immunol. 2008;8(9):726–36.
29. Barlow S, et al. Comparison of human placenta- and bone marrow-derived multipotent mesenchymal stem cells. Stem Cells Dev. 2008;17(6):1095–107.
30. Dehghani L, et al. Safety of intraparenchymal injection of allogenic placenta mesenchymal stem cells derived exosome in patients undergoing decompressive craniectomy following malignant middle cerebral artery infarct, A pilot randomized clinical trial. Int J Prev Med. 2022;13:7.
31. Madani S, et al. Placenta derived mesenchymal stem cells transplantation in type 1 diabetes: preliminary report of phase 1 clinical trial. J Diabetes Metab Disord. 2021;20(2):1179–89.
32. Dominici M, et al. Minimal criteria for defining multipotent mesenchymal stromal cells. The international society for cellular therapy position statement. Cytotherapy. 2006;8(4):315–7.
33. Laurila JP, et al. Human embryonic stem cell-derived mesenchymal stromal cell transplantation in a rat Hind limb injury model. Cytotherapy. 2009;11(6):726–37.
34. Schmuck EG, et al. Biodistribution and clearance of human mesenchymal stem cells by quantitative Three-Dimensional Cryo-Imaging after intravenous infusion in a rat lung injury model. Stem Cells Translational Med. 2016;5(12):1668–75.
35. Miyashita K, et al. Nutraceutical characteristics of the brown seaweed carotenoid Fucoxanthin. Arch Biochem Biophys. 2020;686:108364.
36. Wang X, et al. Fucoxanthin exerts cytoprotective effects against hydrogen Peroxide-induced oxidative damage in L02 cells. Biomed Res Int. 2018;2018:p1085073.
37. Jeong SG, et al. Functional restoration of replicative senescent mesenchymal stem cells by the brown Alga Undaria pinnatifida. Anim Cells Syst (Seoul). 2017;21(2):108–14.
38. Mao H et al. *Fucoxanthin Attenuates Oxidative Damage by Activating the Sirt1/Nrf2/HO-1 Signaling Pathway to Protect the Kidney from Ischemia-Reperfusion Injury.* Oxid Med Cell Longev, 2022. 2022: p. 7444430.
39. Hong DD, et al. Isolation of Fucoxanthin from sargassum oligocystum montagne, 1845 seaweed in Vietnam and its neuroprotective activity. Biomedicines. 2023;11. https://doi.org/10.3390/biomedicines11082310.
40. Lange PS, et al. ATF4 is an oxidative stress-inducible, prodeath transcription factor in neurons in vitro and in vivo. J Exp Med. 2008;205(5):1227–42.
41. Galehdar Z, et al. Neuronal apoptosis induced by Endoplasmic reticulum stress is regulated by ATF4-CHOP-mediated induction of the Bcl-2 homology 3-only member PUMA. J Neurosci. 2010;30(50):16938–48.
42. Teng C, et al. Fucoxanthin ameliorates Endoplasmic reticulum stress and inhibits apoptosis and alleviates intervertebral disc degeneration in rats by upregulating Sirt1. Phytother Res. 2024;38(5):2114–27.
43. Liu S, et al. Autophagy: regulator of cell death. Cell Death Dis. 2023;14(10):648.
44. Young MM, et al. Autophagosomal membrane serves as platform for intracellular death-inducing signaling complex (iDISC)-mediated caspase-8 activation and apoptosis. J Biol Chem. 2012;287(15):12455–68.
45. Mariño G, et al. Self-consumption: the interplay of autophagy and apoptosis. Nat Rev Mol Cell Biol. 2014;15(2):81–94.

Publisher's note